한국통신학회논문지(J-KICS) '13-11 Vol.38C No.11
http://dx.doi.org/10.7840/kics.2013.38C.11.955

부분대역 잡음 재밍 환경에서의 주파수 재할당을 고려한 Link-16 성능 분석

이 규 만◆, 노 홍 준*, 이 종 관*, 임 재 성°

Performance Analysis of Link-16 Waveform considering Frequency Remapping under PBNJ

Kyuman Lee◆, Hongjun Noh*, Jongkwan Lee*, Jaesung Lim°

요 약

합동전술정보분배체계는 미국, 북대서양조약기구 및 기타 연합군에서 운용하고 있는 Link-16의 통신 터미널로 사용된다. 최근 민간 항공분야에서의 교통량 증가로 인해 주파수 수요가 급증함에 따라 Link-16에서 사용 중인 주파수는 다른 시스템에 재할당될 예정이며, 이는 Link-16의 성능에 영향을 미칠 것으로 예상된다. 따라서 본 논문에서는 주파수 대역 감소에 따른 Link-16 성능의 영향을 모의실험과 수치 해석을 통해 기존 성능과 비교하였다. 성능 분석 결과, Nakagami 페이딩과 부분대역 잡음 재밍 환경에서 주파수가 재할당된 Link-16은 성능이 감소됨에도 불구하고 높은 항재밍 능력을 유지하였으며, 동일 시간슬롯에서 다수 사용자들을 지원할 수 있음을 확인하였다.

Key Words : Link-16, frequency remapping, partial-band noise jamming, Nakagami fading, multi-net, anti-jamming

ABSTRACT

The joint tactical information distribution system (JTIDS) is used as the communication terminal of Link-16 by the United States armed forces, north atlantic treaty organization (NATO), and other allied forces. A portion of Link-16 frequencies may be shortly remapped to other systems owing to the growing demand for frequencies, especially in civil aviation, which is witnessing a constant increase in air traffic. This will affect the performance of Link-16. Therefore, in this paper, we analyze the effect of frequency band reduction on the performance of Link-16 waveform under partial-band noise jamming with Nakagami fading, via simulation and numerical analysis. The multi-net and anti-jamming performance of Link-16 with frequency remapping is compared with that of conventional Link-16 systems. The results show that the performance of Link-16 waveform is degraded with the reduction in frequencies. Nonetheless, Link-16 retains its jam resistance, and it can support multiple users in the same time slots.

※ This research was supported by the MSIP(Ministry of Science, ICT & Future Planning), Korea, under the ITRC(Information Technology Research Center) support program supervised by the NIPA(National IT Industry Promotion Agency) (NIPA-2013-(H0301-13-2003)).
◆ First Author : 아주대학교 컴퓨터공학과 국방전술네트워크 연구센터, mool717@ajou.ac.kr, 정회원
° Corresponding Author : 아주대학교 소프트웨어융합학과 국방전술네트워크 연구센터, jaslim@ajou.ac.kr, 종신회원
* 아주대학교 국방전술네트워크 연구센터, nonoboy@ajou.ac.kr, jklee64@ajou.ac.kr, 정회원
논문번호 : KICS2013-08-348, 접수일자 : 2013년 8월 26일, 최종논문접수일자 : 2013년 11월 4일

Ⅰ. INTRODUCTION

Network-centric warfare (NCW) is a doctrine that is adopted in military operations by using modern communication systems. NCW employs networking concepts to increase data rate and situational awareness[1]. Tactical data links (TDLs) are key elements of NCW. They are used to transmit and receive tactical data, thereby providing weapon system effectiveness, interoperability, real-time exchange of information among combat personnel, and the capability to command and control military operations. Moreover, TDLs must provide robust information management in adverse operation environments[3]. Link-16 is a TDL used by the U.S. armed forces, NATO, and other allied forces. The joint tactical information distribution system (JTIDS) is a component of Link-16 that provides the functions required for NCW. Link-16 is a jam-resistant TDL, and it can be configured in multi-net mode to support several operations simultaneously.

Air traffic is rapidly increasing on a global scale. Hence, new airports are being built and existing ones are being extended to accommodate more traffic. With the increase in air traffic, there is a growing demand for the already scarce frequencies for air traffic control and other safety services[5].

The spectrum required for military radio systems is often unused because of occasional operation[6]. This has influenced the opinion that these bands can be utilized with existing systems to manage the increase in air traffic, which can be achieved by sharing bands already used by other similar services or subdividing existing bands and migrating existing services to a new sub-band. However, sharing bands is not feasible because it may cause significant interference among different systems, thereby degrading the communication environment; a rule is required to prevent such a scenario. Link-16 uses 51 discrete frequencies from 960 MHz to 1215 MHz, which are known as golden bands. US frequency spectrum authorities have reallocated the lower 14 JTIDS frequencies for other uses[7]. Moreover, the Link-16 frequency may have to be dropped because of plans to employ the L5 frequency for civilian band of global positioning system (GPS) services.

The performance of Link-16 waveform under interference and fading has been investigated in previous studies[2-4]; however, most studies focused on pulsed-noise interference (PNI), and they did not consider the frequency remapping of Link-16. In this paper, we analyze the effect of frequency band reduction on Link-16 performance when a portion of Link-16 frequencies is used by other systems. This is achieved via analysis of multi-net and anti-jamming performance under Nakagami fading with partial-band noise (PBN) jamming.

The remainder of this paper is organized as follows. The system model is introduced in Section II. Link-16 multi-net and anti-jamming performance is analyzed in Sections III and IV, respectively. Finally, we conclude the paper in Section V.

Ⅱ. SYSTEM MODEL DESCRIPTION

2.1. JTIDS Transmitter and Receiver

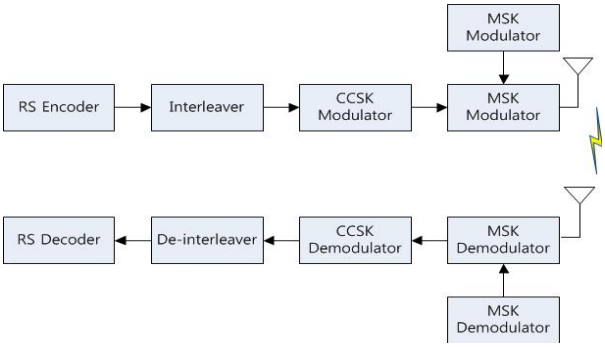

Fig. 1. Model of Link-16 transmitter and receiver

Link-16 uses the ultra high frequency (UHF) band, and it is specifically designed to resist interference effectively. The Link-16 waveform can be understood on the basis of the transmission and reception structure of JTIDS. As shown in Figure 1, the JTIDS system consists of a Reed-Solomon (RS) encoder, an interleaver, a cyclic code-shift keying

(CCSK) 32-ary modulator, a frequency hopping module, a minimum-shift keying (MSK) modulator, and an RF channel[8]. The receiver performs the inverse process of the transmitter[4].

The original message stream of Link-16 is divided into 5-bit symbols for channel coding. Each data symbol is encoded by the RS encoder using the (31, 15) code, and the header symbol is (16, 7). The encoded header and data symbols are interleaved for transmission security. After interleaving, Link-16 produces a 32-chip sequence using the 32-ary CCSK modulator in order to represent each 5-bit symbol. Next, the 32-chip sequence is scrambled for secure transmission, and the MSK modulator modulates this chip sequence before transmission. Each pulse signal modulated by the MSK modulator is transmitted, yielding 51 carrier frequencies according to a hopping pattern. This pattern makes it difficult for a jammer to attack because the frequency that is used cannot be determined. The received symbol is determined via cross-correlation; a symbol with a large cross-correlation value is selected.

Link-16 supports two structures, single-pulse and double-pulse, according to the packing structure. The pulse signal is transmitted once and twice per symbol in the single-pulse and double-pulse structures, respectively. Thus, by using the frequency-hopping pattern in the double-pulse structure, Link-16 can achieve diversity gain in the frequency and time domains.

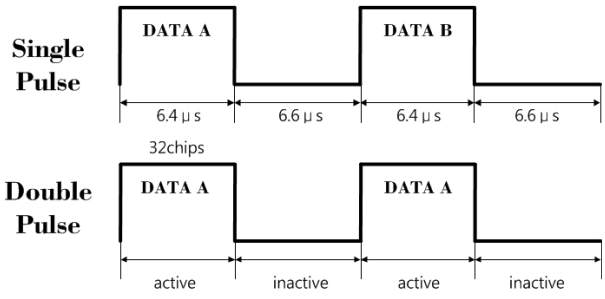

Fig. 2. Pulse structure of Link-16

Figure 2 shows the signal transmission type of Link-16. After the transmission of a single pulse, Link-16 remains idle for frequency hopping; therefore, in the double-pulse structure, two pulse signals are passed through different frequency bands at different times.

2.2. Multi-net

Link-16 operates on the basis of frequency hopping (FH) and time division multiple access (TDMA). FH is a function of a variable called a net number, which permits various users to use the same time slots to exchange data. Link-16 uses 128 defined nets according to hopping patterns as shown in Figure 3[9]. Many users can use the same time slots with different net numbers, and a terminal can operate on different nets from slot to slot; however, any one terminal can operate on only one net for any given time slot. If many units use their time slots heavily in the multi-net, pulses from two or more multi-netted transmitters may occasionally collide at a given receiving terminal.

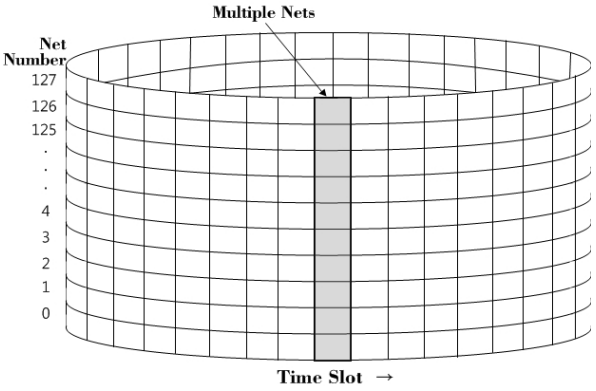

Fig. 3. Multi-net structure

2.3. Jammer Model

PBN jamming is used for the anti-jamming performance analysis of Link-16. In this study, we assume that the jammer knows the frequency band and channel bandwidth used by Link-16; however, it is difficult to determine the frequency-hopping pattern and starting point of a time slot. These assumptions are based on the fact that the Link-16 model is well known, and the hopping pattern and encryption technique are changed regularly[8]. The hopping pattern is a function of a cryptographic key.

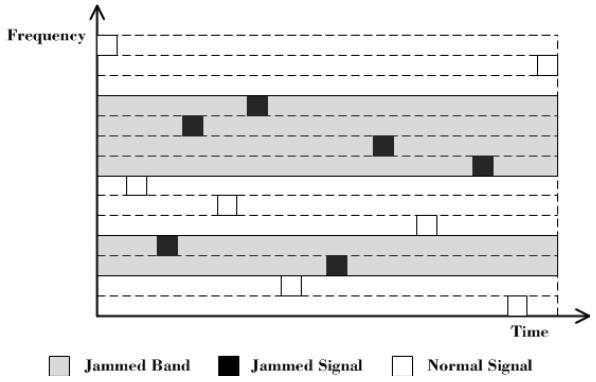

Fig. 4. PBN jammer model

A PBN jammer can concentrate its power over a fraction of the total bandwidth instead of spreading its power over all the frequency bands used by a system[9]. The fraction ρ_B whose performance is affected by the jammer is given by[16]

$$\rho_B = \frac{B_J}{B_T}, \quad (1)$$

where B_J is the jamming bandwidth and B_T is the total bandwidth. The jamming efficiency can be improved by concentrating to the specific bands. Thus, the desired signal is affected for only a fraction of the time; however, if the ratio of packets corrupted by interference is higher than the error correction capability, the packet may be lost. To avoid a PBN jamming attack, it is necessary to employ robust forward error correction (FEC) with the interleaving of code symbols over a sufficiently large number of hops. As shown in Figure 4, the shaded frequency bands are jammed by a PBN jammer. Without a cryptographic key, the jammer cannot determine the frequency to be jammed, and it can jam only a few frequencies. Thus, owing to the limited jamming power, the power of the jamming signal is diminished if the jamming bands are widened.

In the double-pulse structure, diversity gain can be achieved in the frequency domain because two symbols are transmitted through different frequencies. In this study, the received signal is decoded by using the selection combining (SC) for multi-net performance analysis and maximum ratio combining (MRC) techniques for anti-jamming performance analysis. The SC technique selects the strongest received signal, whereas the gain of each channel is made proportional to the rms signal level and inversely proportional to the mean square noise level of the channel in the MRC technique.

Ⅲ. MULTI-NET PERFORMANCE ANALYSIS

Because the multi-net performance depends on the number of users who can use a time slot simultaneously, it plays an important role in determining the options available for combat operations. In Link-16, multiple access interference (MAI) causes mutual interference, which inevitably occurs because of colliding pulses from different nets. This is because Link-16 defines 128 hopping patterns in 51 discrete frequencies, and not all patterns can be orthogonal. The probability of collision between transmitted signals increases with the number of nets existing at the same frequency. In this section, we show the effect of dividing Link-16 frequencies on multi-net performance, and we examine the possibility of conducting operations by determining the maximum feasible number of multi-nets.

3.1. Simulation Parameters

We evaluated the multi-net performance of Link-16 waveform by using a MATLAB simulator. The simulation parameters are listed in Table 1.

A Link-16 terminal provides 200 W in the normal power mode. We use this value in the simulation, and we assume that the transmission distance between the transmitter and the receiver is 555.6 km (300 NM), considering the normal range of Link-16.

Table 1. Simulation Parameters

Parameters	Values
Transmission Power	200 W
Transmission distance	555.6 km
Bandwidth	3 MHz
Frequency hopping rate	77,000/s
Type of MAI	Asynchronous interference
Combining techniques	SC
Channel model	Two-ray, Nakagami Fading
Channel coding	RS code(31,15)
Detection	Coherent detection

The Link-16 frequencies are spaced at intervals of 3 MHz, except for two gaps of 22 MHz and 25 MHz either side of 1030 MHz and 1090 MHz, used by the identification, friend or foe (IFF) and selective identification feature (SIF) systems[11]. To preclude jamming by a narrow band jammer, the Link-16 transmitter/receiver changes frequencies up to 77,000 times per second within each time slot. Because the frequency-hopping time is extremely small as compared to the transmission delay, it is not possible to synchronize all nodes at the receiver. Therefore, we assume that the type of MAI is asynchronous interference. We employ a two-ray channel model, which considers line-of-sight (LOS) signals and reflected signals from the ground[4].

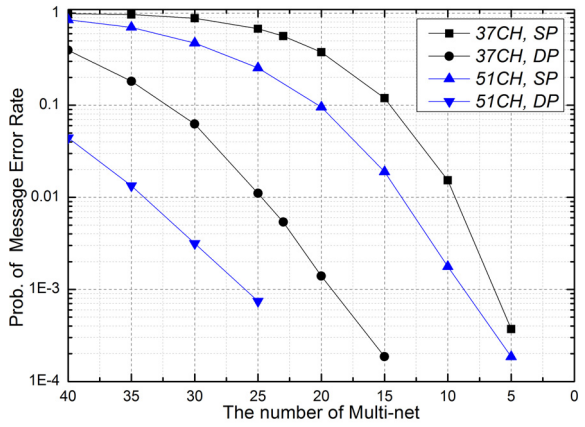

Fig. 5. Link-16 multi-net performance analysis via simulation

3.2. Simulation Results

We considered the worst-case scenario, wherein the neighboring nodes that cause interference are situated within 1 km. In Link-16, multiple users can tolerate interference in data transmission in the same slots before they experience a 1% received message error rate (MER)[12]. Therefore, we observed a probability of message error, $P_M = 10^{-2}$, and we derived the number of available multi-nets. The results are tabulated below.

Table 2. Possible Number of multi-nets

Total Bandwidth	Single Pulse	Double Pulse
51 CH	13	33
37 CH	9	24

Table 2 shows the multi-net performance in the single-pulse and double-pulse structures. To receive more than 99% of the messages, Link-16, which remaps frequencies, should operate less than 9 multi-nets; conventional Link-16 systems can operate 13 multi-nets in the single-pulse structure. The double-pulse structure outperforms the single-pulse structure. In Table 2, we can see that the less than 24 multi-nets need to be configured in order to receive more than 99% of the messages. However, the double pulse has a disadvantage in throughput because it transmits data twice by duplicating messages. Thus, performance degradation is observed. In general, Link-16 requires 4 multi-nets for a single mission; hence, we conclude that it can support operations in spite of performance degradation.

Ⅳ. ANTI-JAMMING PERFORMANCE ANALYSIS

In this paper, two approaches were adopted for anti-jamming performance analysis. First, we analyzed Link-16 performance using a numerical method, and we compared the results with those of the simulation.

4.1. Probability of Channel Chip Error

As explained above, Link-16 uses an MSK demodulator to recover the scrambled 32-chip sequence and a CCSK demodulator to detect the original 5-bit symbol. The MSK channel chip error performance, which is similar to that of binary phase-shift keying (BPSK) and quadrature phase-shift keying (QPSK) in additive white Gaussian noise (AWGN)[13], is given by

$$p_c = Q\left(\sqrt{\frac{2E_c}{N_0}}\right), \quad (2)$$

where $Q(\bullet)$ is the Q function and E_c is the average energy per chip. One symbol consists of 5 bits and it is converted into a 32-chip sequence. In addition, Link-16 uses an FEC code. Thus, (2) can be expressed as

$$p_c = Q\left(\sqrt{\frac{10rE_b}{32N_0}}\right), \quad (3)$$

where E_b is the average energy per bit and r is the code rate of 15/31.

When we apply Nakagami fading to (3), we get the probability of channel chip error with no jamming for single-pulse structure, $p_{c_{S0}}$, as follows:

$$p_{c_{S0}} = \int_0^\infty Q\left(\sqrt{\frac{10rE_b a^2}{32N_0}}\right) f_X(a^2)da^2, \quad (4)$$

where a is the channel gain of the received signal, and f_X is modeled as a Nakagami random variable with a probability density function (pdf) [14] given by

$$f_X(\alpha) = \frac{2}{\Gamma(m)}\left(\frac{m}{\Omega}\right)^m \alpha^{2m-1} e^{\left(-m\frac{\alpha^2}{\Omega}\right)}, \alpha \geq 0 \quad (5)$$

where $\Omega = E(\alpha^2)$ is the average fading power, m is the Nakagami fading parameter ($m \geq 1/2$), and $\Gamma(\bullet)$ is the Gamma function. The purpose of this paper is the comparison of performance when the frequency bands of Link-16 are remapped to other systems. Futhermore JTIDS is operated in the UHF band (LOS is required) [4]. Thus, we set the Nakagami fading figure, m, to 2 in the numerical analysis and simulation.

If jamming occurs in the channels, the probability of the channel chip error is converted into the signal to interference and noise ratio (SINR), which is calculated in a similar manner as the signal to noise ratio (SNR) by considering the interference due to jamming. Here, the jamming signal is modeled as undergoing the same fading. When the jamming signal energy is N_J, the probability of channel chip error, $p_{c_{S1}}$ [16], is given by (6), where c is channel gain of jamming signal and B_J is the number of jamming bands. In equation (6), the jamming signal energy is divided by the number of jamming bands to compare fairly the performance of Link-16 with frequency remapping with that of conventional Link-16 systems. This means that there is an one jammer and the jamming power of each jammed channel is the same. Thus, the only difference between two systems is the number of total bands.

In the double-pulse structure, three cases are considered for the two received signals because of jamming.

1) Both signals do not undergo jamming.
2) One signal undergoes jamming, whereas the other does not.
3) Both signals undergo jamming independently.

We assume that PBN jammer attacks each bands with the same power and a level of jamming signal is much higher than a normal signal. This means that decoding a signal that has not been jammed is more effective when the one of two symbols undergoes jamming. Thus we use the MRC technique with weight factor of 1 for the second cases, and with weight factor of 0.5

$$p_{c_{S1}} = \int_0^\infty \int_0^\infty Q\left(\sqrt{\frac{10rE_b a^2}{32\left(N_0 + c^2\frac{N_J}{B_J}\right)}}\right) f_X(a^2) f_X(c^2) da^2 dc^2 \quad (6)$$

$$p_{c_{D0}} = \int_0^\infty \int_0^\infty Q\left(\sqrt{\frac{10rE_b(a^2+b^2)}{32N_0}}\right) f_X(a^2) f_X(b^2) da^2 db^2 \quad (7)$$

$$p_{c_{D1}} = \int_0^\infty \int_0^\infty \int_0^\infty \int_0^\infty Q\left(\sqrt{\frac{10rE_b}{32}\left(\frac{a^2}{N_0 + \frac{c_1^2 N_J}{B_J}} + \frac{b^2}{N_0 + \frac{c_2^2 N_J}{B_J}}\right)}\right) f_X(a^2) f_X(b^2) f_X(c_1^2) f_X(c_2^2) da^2 db^2 dc_1^2 dc_2^2 \quad (8)$$

for the first and third case in the performance analysis. Because the MRC technique with weight factor of 1 decodes a signal that has not been jammed, the probability of channel chip error for the double-pulse structure is the same as that for the single-pulse structure.

Using the MRC technique with weight factor of 0.5, the probability of channel chip error for the first case, $p_{c_{D0}}$, is given by (7), where b is the channel gain of the second received symbol. $D0$ of $p_{c_{D0}}$ denotes double pulse with no jamming.

$p_{c_{D1}}$ in equation (8) is the probability of channel chip error when both received signals undergo jamming independently. Thus, the each received jamming signal is affected by different channel gains, c_1 and c_2.

4.2. Performance Analysis of PBN Jamming

Because we assume that a jammer knows the system bandwidth of Link-16, the symbols in the jamming band are affected by jamming. We consider two cases, i.e., with and without jamming; the probability of each channel symbol error[4] is given by

$$p_{s_i} \le \sum_{j=0}^{32} \zeta_{UB_j} \binom{32}{j} p_{c_i}^j (1-p_{c_i})^{32-j}, \quad i = S0, S1, D0, D1, \quad (9)$$

where ζ_j are the conditional probabilities of channel symbol errors when $N=j$ chip errors occur. In this paper, the ζ_{UB_j} which is a tight upper bound of the channel symbol error probability from the analytical results is used to analyze the performance of JTIDS[15].

The probability of channel symbol error according to the presence of jamming is given by (9). The probability of symbol error for the entire system under PBN jamming is obtained by averaging (9). Thus, we get

$$SP: p_s = (1-\rho_B) p_{s_{S0}} + \rho_B p_{s_{S1}}$$
$$DP: p_s \le (1-\rho_B)^2 p_{s_{D0}} + 2(1-\rho_B)\rho_B p_{s_{S0}} + \rho_B^2 p_{s_{D1}}. \quad (10)$$

Now, from (9) and (10) with $r = 15/31$ and ζ_{UB_j}, we get the probability of symbol error of Link-16 for the single-pulse and double-pulse structures under PBN jamming with Nakagami fading[4].

$$P_S \approx \frac{1}{n} \sum_{e=t+1}^{n} e\binom{n}{e} p_s^e (1-p_s)^{(n-e)} \quad (11)$$

where e denotes the number of symbols with an error of 31 symbols. Link-16 decodes data via RS coding, and this RS (n, k) code can correct errors up to $t = (n-k)/2$[16].

4.3. Numerical Results

Figures 6 and 7, where $m=2$ and $E_b/N_0=10$ dB show the probability of symbol error of Link-16 according to the equation (10) and (11).

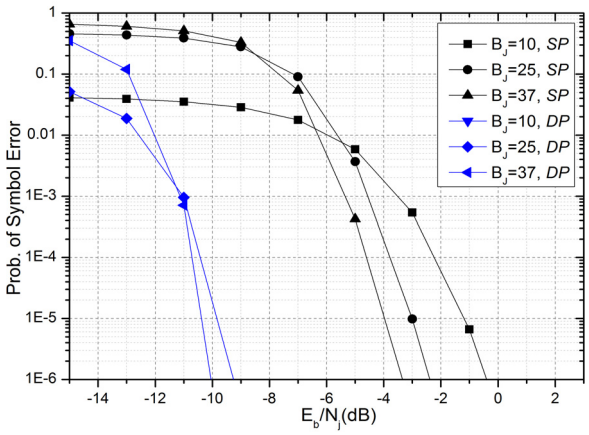

Fig. 6. Probability of symbol error of Link-16 via numerical analysis under PBN jamming with Nakagami fading, where $B_T=51$

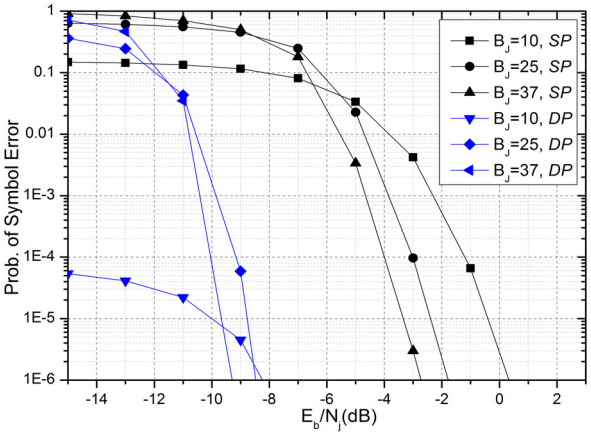

Fig. 7. Probability of symbol error of Link-16 via numerical analysis under PBN jamming with Nakagami fading, where $B_T=37$

The anti-jamming performance is degraded when the frequencies of Link-16 are remapped to 37 frequencies. For example, in Figure 7, where $B_J=25$ for the double-pulse structure, we can obtain a probability of symbol error lower than 10^{-5} when E_b/N_j is greater than -9 dB, whereas it is more than -10 dB in Figure 6. In normal system, a system is designed to transfer higher power than threshold for ensuring a probability of symbol error. Thus, the degradation about 1 dB of received signal is not severe, even if the jamming bands constitute more than half of the entire band, because the difference of the number of entire bands which affect the performance of the two Link-16 waveforms using existing frequencies and remapping frequencies is small. Furthermore, the double-pulse structure outperforms the single-pulse structure by 6 dB at $P_s=10^{-5}$ for $B_J=25$. In this reason, the probability of symbol error of double-pulse structure for $B_J=10$ is not shown in Figure 6.

4.4. Simulation Results

The parameters used for anti-jamming performance analysis are nearly identical to those used for multi-net performance analysis, except for transmission power, jammer and combining technique. We investigate the probability of symbol error at $E_b/N_0=10$ dB instead of using the actual transmission power of the Link-16 terminal. We assume that a PBN jammer concentrates its power on a portion of bands of Link-16. 10, 25, and 37 jamming bands are equally considered for comparison under the same conditions, even though the total number of bands is different.

Figures 8 and 9 show the performance of two Link-16 waveforms for different jamming bands under PBN jamming with Nakagami fading for coherent demodulation, where E_b/N_0 is fixed at 10 dB. As well as numerical analysis, the anti-jamming performance is degraded about 1 dB when the frequencies of Link-16 are remapped to 37 frequencies. Since the difference of total number of frequencies used by two Link-16 waveforms is not large, the impact on performance is small.

Futhermore we can see that the simulation results are slightly better than the numerical results, because the tight upper bound of the conditional probabilities of channel symbol error, ζ_{UB_j}, is used for numerical analysis. This means that we consider the worst communication environment, and it results in poorer performance.

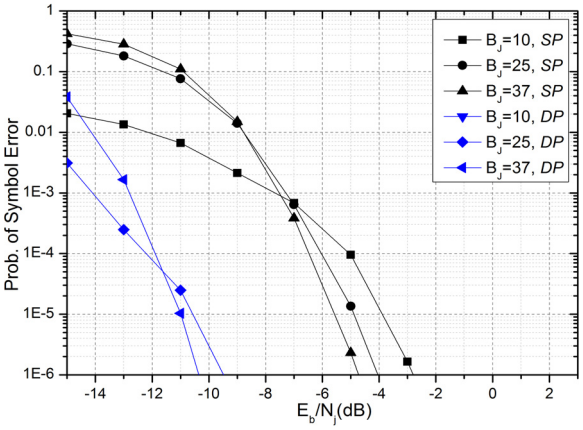

Fig. 8. Probability of symbol error of Link-16 via simulation under PBN jamming with Nakagami fading, where $B_T = 51$

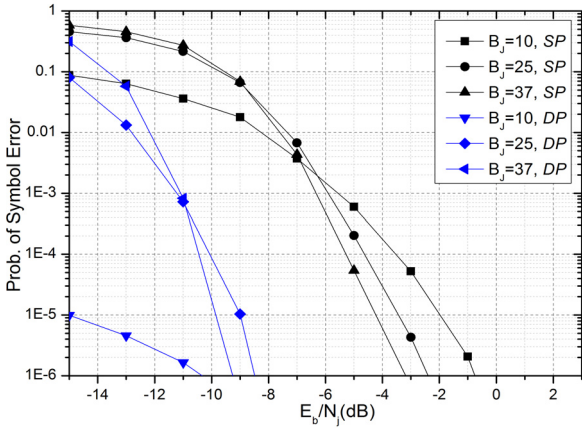

Fig. 9. Probability of symbol error of Link-16 via simulation under PBN jamming with Nakagami fading, where $B_T = 37$

In the numerical analysis, the anti-jamming performance of Link-16, which used less than 51 frequency bands, is degraded because the probability of avoidance of jamming increases as many frequencies are used. This can be observed in the simulations results as we expected. For example, in Figures 8 and 9, when the number of jamming bands is 10 for single-pulse structure, the difference in performance is greater than 1.5 dB. On the other hand, when more than half of the total bands are jammed, the degradation is less than 1.5 dB. This result shows that if ρ_B is greater than 0.5, the difference in performance is not significant because many frequencies are already affected by the interference due to the jammer. Moreover, the probability of chip error decreases as E_b/N_j increases, because the jamming power is reduced as many frequency bands are jammed.

V. CONCLUSION

In this study, we investigated the probability of symbol error and the number of available multi-nets for Link-16 by considering frequency remapping. Through the numerical analysis and extensive simulation, we arrived at the following conclusions. First, the anti-jamming performance of Link-16 is degraded with the reduction in frequencies. As the performance degradation is around 1-2 dB, Link-16 retains its jam resistance. Second, the double-pulse structure outperforms the single-pulse structure under PBN jamming with Nakagami fading by transmitting the same messages twice through different frequencies. Third, the simulation results are better than the numerical results because of the assumption of the upper bound; nonetheless, both results exhibit similar trends. Finally, the number of multi-nets is sufficient for performing operations when the frequencies of Link-16 are remapped.

References

[1] C. Wilson, *Network centric operations: Background and Oversight Issues for Congress*, CRS Report for Congress, Mar. 2007.

[2] H. Wang, J. Kuang, Z. Wang, and H. Xu, “Transmission performance evaluation of JTIDS,” in *Proc. IEEE Military Commun. Conf. (MILCOM)*, vol. 4, pp. 2264-2268, Atlantic City, U.S.A., Oct. 2005.

[3] D. Lekkakos and C. Robertson, “Performance analysis of a LINK-16/JTIDS compatible waveform transmitted over a channel with pulse-noise interference,” in *Proc. IEEE Pacific Rim Conf.*, pp. 29-34, Victoria, Canada, Aug. 2009.

[4] C.-H. Kao, F. Kragh, and C. Robertson, “Performance analysis of a JTIDS

/Link-16-type waveform transmitted over Nakagami fading channels with pulsed-noise interference," in *Proc. IEEE Military Commun. Conf. (MILCOM)*, pp. 1-6, San Diego, U.S.A., Nov. 2008.

[5] LS telcom, *Aeronautical spectrum and frequency management solutions*, retrieved from http://www.lstelcom.com/fileadmin/content/marketing/brochures/aeronautical_brochure_highres.pdf

[6] L. Berleman and S. Mangold, *Cognitive Radio and Dynamic Spectrum Access*, John wiley & Sons Ltd, July 2009.

[7] DTIC, *LINK 16 Electromagnetic Compatibility (EMC) Features Certification Process and Requirements (DoD 4650.1-R1)*, retrieved Apr., 26, 2005, from http://www.dtic.mil/whs/directives/corres/pdf/465001r1p.pdf.

[8] H. J. Noh, J. B. Kim, J. S. Lim, J. H. Nam, and D. W. Jang, "Anti-jamming performance analysis of Link-16 waveform," *J. Korean Inst. Commun. Inform. Sci. (KICS)*, vol. 35, no. 12, pp. 1105-1112, Dec. 2010.

[9] *Understanding Link-16: A Guidebook for New User*, Northrop Grumman Corporation, Sep. 2001.

[10] R. A. Poisel, *Modern Communications Jamming Principles and Techniques*, Artech House, Dec. 2004.

[11] R. Sabatini, L. Aulanier, G. L. marinoni, M. Martinez, B. Pour, and H. Rutz, *Multifunctional Information Distribution System (MIDS) Low Volume Terminal (LVT) development and integration programs towards LINK-16 network centric allied/coalition operations*, retrieved Oct. 2011, from http://ftp.rta.nato.int/public/PubFullText/RTO/MP/RTO-MP-IST-083/MP-IST-083-11.doc.

[12] R. Ghanadan, P. Tufano, J. Hsu, J. Gu, and C. Connelly, "Flexible access secure transfer (FAST) tactical communications waveform for airborne networking," in *Proc. IEEE Military Commun. Conf. (MILCOM)*, vol. 2, pp. 1167-1173, Atlantic City, U.S.A., Oct. 2005.

[13] S. Pasupathy, "Minimum shift keying: a spectrally efficient modulation," *IEEE Commun. Mag.*, vol. 17, no. 4, pp. 14-22, July 1979.

[14] S. M. Rytov, Y. A. Kravtsov, and V. I. Tatarskii, *Principle of Statistical Radio physics I*, Springer-Verlag, July 1987.

[15] C.-H. Kao, C. Robertson, and K. Lin, "Performance analysis and simulation of cyclic code-shift keying," in *Proc. IEEE Military Commun. Conf. (MILCOM)*, pp. 1-6, San Diego, U.S.A., Nov. 2008.

[16] J. G. Proakis, *Digital Communications*, 4th ed., McGraw Hill, Aug. 2000.

[17] H. J. Noh and J. S. Lim, "Partitioned cyclic code shift keying for JTIDS," in *Proc. IEEE Military Commun. Conf. (MILCOM)*, pp. 1-6, Orlando, U.S.A., Oct.-Nov. 2012.

이 규 만 (Kyuman Lee)

2011년 2월 아주대학교 전자공학과 졸업

2011년 3월~현재 아주대학교 컴퓨터공학과 석박사 통합과정

<관심분야> 위치인식, 전술데이터링크 웨이브폼

노 홍 준 (Hongjun Noh)

2008년 2월 아주대학교 정보및 컴퓨터 공학과 졸업

2008년 3월~현재 아주대학교 컴퓨터공학과 석박사 통합과정

<관심분야> 항공/위성 통신

이 종 관 (Jongkwan Lee)

2000년 2월 육군사관학교 전자공학과 졸업
2004년 2월 한국과학기술원 전기 및 전자공학과 석사
2011년 3월~현재 아주대학교 NCW공학과 박사 과정
<관심분야> Dynamic TDMA, Ad-hoc Network

임 재 성 (Jaesung Lim)

1983년 2월 아주대학교 전자공학과 졸업
1985년 2월 한국과학기술원 영상통신 석사
1985년 2월 한국과학기술원 디지털통신 박사
1998년 3월~현재 아주대학교 소프트웨어융합학과 교수
<관심분야> 이동 및 위성통신, 무선네트워크, 국방전술통신